

P-PROCESS NUCLEOSYNTHESIS INSIDE SUPERNOVA-DRIVEN SUPERCRITICAL ACCRETION DISKS

SHIN-ICHIROU FUJIMOTO

Department of Electronic Control, Kumamoto National College of Technology, Kumamoto 861-1102, Japan;
fujimoto@ec.knct.ac.jp

MASA-AKI HASHIMOTO AND OSAMU KOIKE

Department of Physics, School of Sciences, Kyushu University, Fukuoka 810-8560, Japan;
hashi@gemini.rc.kyushu-u.ac.jp, koike@gemini.rc.kyushu-u.ac.jp

AND

KENZO ARAI AND RYUICHI MATSUBA

Department of Physics, Kumamoto University, Kumamoto 860-8555, Japan; arai@sci.kumamoto-u.ac.jp,
matsuba@sci.kumamoto-u.ac.jp

Draft version September 29, 2018

ABSTRACT

We investigate p-process nucleosynthesis in a supercritical accretion disk around a compact object of $1.4 M_{\odot}$, using the self-similar solution of an optically thick advection dominated flow. Supercritical accretion is expected to occur in a supernova with fallback material accreting onto a new-born compact object. It is found that appreciable amounts of p-nuclei are synthesized via the p-process in supernova-driven supercritical accretion disks (SSADs) when the accretion rate $\dot{m} = \dot{M}c^2/(16L_{\text{Edd}}) > 10^5$, where L_{Edd} is the Eddington luminosity. Abundance profiles of p-nuclei ejected from SSADs have similar feature to those of the oxygen/neon layers in Type II supernovae when the abundance of the fallback gas far from the compact object is that of the oxygen/neon layers in the progenitor. The overall abundance profile is in agreement with that of the solar system. Some p-nuclei, such as Mo, Ru, Sn, and La, are underproduced in the SSADs as in Type II supernovae. If the fallback gas is mixed with a small fraction of proton through Rayleigh-Taylor instability during the explosion, significant amounts of ^{92}Mo are produced inside the SSADs. ^{96}Ru and ^{138}La are also produced when the fallback gas contains abundant proton though the overall abundance profile of p-nuclei is rather different from that of the solar system. The p-process nucleosynthesis in SSADs contributes to chemical evolution of p-nuclei, in particular ^{92}Mo , if several percents of fallback matter are ejected via jets and/or winds.

Subject headings: Accretion, accretion disks — nuclear reactions, nucleosynthesis, abundances — stars: supernovae: general

1. INTRODUCTION

There exist 35 neutron deficient stable nuclei with mass number $A \geq 74$ referred to as p-nuclei. These nuclei are found in meteorites only inside the solar system; isotopic anomalies involving these nuclei are also found in some primitive meteorites. Many production sites of the p-nuclei have been proposed: oxygen/neon layers of highly evolved massive stars during their presupernova phase (Arnould 1976) and during their supernova explosion (Woosley & Howard 1978); X-ray novae (Schatz et al. 1998); neutrino-driven winds originated from a nascent neutron star shortly after supernova explosion (Hoffman et al. 1996); Type Ia supernova explosion (Howard, Meyer & Woosley 1991); helium-accreting CO white dwarfs of sub-Chandrasekhar mass (Goriely et al. 2002). Among them, the most promising is the oxygen/neon layers during Type II supernova explosion. The p-nuclei are synthesized by the photodisintegrations of s-nuclei (s-process seeds) produced in the layers during the core helium burning in the progenitor. Photodisintegrate (γ, n) reactions are followed by (γ, p) and/or (γ, α) reactions. The production of p-nuclei via the subsequent photodisintegrations is referred to as a p-process. Extensive investigations of the p-process in Type II supernovae are performed by Prantzos et al. (1990b), Rayet, Prantzos & Arnould (1990), Rayet et

al. (1995), and Arnould, Rayet & Hashimoto (1998) with a large nuclear network. A p-process model of Rayet et al. (1995) in the oxygen/neon layers during Type II supernovae reproduces the overall abundance profile of p-nuclei in the solar system. However, the model has a conspicuous shortcoming of underproduction of $^{92,94}\text{Mo}$, $^{96,98}\text{Ru}$, and ^{138}La . Abundant productions of such p-nuclei have been invoked to neutrino processes (Woosley et al. 1990; Goriely et al. 2001); Yield of ^{138}La in the oxygen/neon layers is increased via neutrino interactions though those of Mo and Ru are not appreciably changed (Goriely et al. 2001). Enhancement of s-process seeds synthesized in the layers during core helium burning could improve the underproduction of Mo and Ru with an extremely high rate of $^{22}\text{Na}(\alpha, n)^{25}\text{Mg}$ reaction (Costa et al. 2000). However, such a high rate is possibly excluded by a recent experiment (Jaeger et al. 2001).

During supernova explosion in massive stars, certain fraction of ejected matter is expected to fall back onto a new-born compact object with supercritical accretion rates greater than $10^4 \dot{M}_{\text{cr}}$ (Woosley & Weaver 1995, hereafter WW95), where \dot{M}_{cr} is the critical mass accretion rate given by $16L_{\text{Edd}}/c^2$ with the Eddington luminosity, L_{Edd} . If the fallback material has substantial angular momentum, formation of an accretion disk is inevitable (Mineshige et

al. 1997). Fujimoto et al. (2001) have investigated nucleosynthesis inside supernova-driven supercritical accretion disks (SSADs) and shown that appreciable nuclear reactions take place if the accretion rate $\dot{M} > 10^5 \dot{M}_{cr}$. At such high accretion rates, SSADs contain the regions where density, temperature, and dynamical time-scale are comparable to those of the oxygen/neon layers in Type II supernovae. Therefore, the p-process is likely to operate efficiently inside SSADs.

We propose a SSAD as a candidate for the production of p-nuclei. In §2, we present a model of SSADs and a nuclear network to calculate the abundance evolution inside a SSAD. We also discuss possible progenitors for p-process nucleosynthesis inside SSADs and the initial chemical abundances of the fallback material far from the central compact remnant. In §3, we describe abundance distributions of p-nuclei inside SSADs, ejected masses of these nuclei from SSADs, and effects of proton and helium contamination of the fallback gas via Rayleigh-Taylor instability. We discuss our results in §4 and finally present concluding remarks in §5.

2. MODEL AND INPUT PHYSICS

2.1. The Supercritical Accretion Disk Model

Physical quantities of supercritical accretion disks with $\dot{M} \gg \dot{M}_{cr}$ are well described in terms of the self-similar solution. The density ρ , temperature T and drift time-scale t_{dr} of accreting gas are evaluated with the self-similar disk model as adopted by Fujimoto et al. (2001) to be

$$\left(\frac{\rho}{10^4 \text{ g cm}^{-3}}\right) = 1.9(1 + \alpha_{vis}^2/7) \left(\frac{M}{1.4M_{\odot}}\right)^{-1} \times \left(\frac{\alpha_{vis}}{0.01}\right)^{-1} \left(\frac{\dot{m}}{10^6}\right) \left(\frac{r}{3r_g}\right)^{-3/2}, \quad (1)$$

$$\left(\frac{T}{10^9 \text{ K}}\right) = 4.3 \left(\frac{M}{1.4M_{\odot}}\right)^{-1/4} \times \left(\frac{\alpha_{vis}}{0.01}\right)^{-1/4} \left(\frac{\dot{m}}{10^6}\right)^{1/4} \left(\frac{r}{3r_g}\right)^{-5/8}, \quad (2)$$

$$\left(\frac{t_{dr}}{0.01 \text{ s}}\right) = 1.9\sqrt{1 + \alpha_{vis}^2/7} \left(\frac{M}{1.4M_{\odot}}\right) \times \left(\frac{\alpha_{vis}}{0.01}\right)^{-1} \left(\frac{r}{3r_g}\right)^{3/2}, \quad (3)$$

where r is the radial coordinate, M is the mass of the central compact object, α_{vis} is the viscous parameter, $\dot{m} = \dot{M}/\dot{M}_{cr}$, and $r_g = 2GM/c^2$ is the Schwarzschild radius. The model has been assumed to be steady and axisymmetric with the self-gravity ignored. It is noted that in SSADs with $\dot{m} \lesssim 10^{12}$ advective cooling dominates over radiative and neutrino cooling; it balances with viscous energy generation. A disk is also assumed to be extended from the last stable circular orbit around a black hole to the location of accretion shock $\sim 10^9$ cm (Fryer, Colgate & Pinto 1999; MacFadyen, Woosley & Heger 2001). Hence, the inner and outer boundaries of the disk, r_{in} and r_{out} , are set to be $3r_g$ and $3 \times 10^3 r_g (= 1.2 \times 10^9 M/M_{\odot} \text{ cm})$, respectively. A sequence of the models is specified in terms

of M , α_{vis} , and \dot{m} . In the present paper, we fix both $M = 1.4 M_{\odot}$ and $\alpha_{vis} = 0.01$ (e.g. Hawley 2000), while \dot{m} is left to be a parameter.

2.2. The Nuclear Reaction Network

We have developed a nuclear reaction network which has been extended from a smaller network (Hashimoto & Arai 1985; Koike et al. 1999). The nuclear data are taken from the data base REACLIB¹, which includes many experimental rates and theoretical Hauser-Feshbach rates (Rauscher & Thielemann 2000, 2001). We have also used the experimental mass data (Audi & Wapstra 1995). The reactions included in the network are (n, γ) , (n, p) , (n, α) , (p, γ) , (p, α) , (α, γ) , 3α , and their inverse reactions. The various channels of $^{12}\text{C} + ^{12}\text{C}$, $^{12}\text{C} + ^{16}\text{O}$, and $^{16}\text{O} + ^{16}\text{O}$ are also included in the network. For β^- and β^+ decays, REACLIB rates are updated with the corresponding data in Horiguchi et al. (1996) if available. We have also added β^- and β^+ decays and electron and positron captures (Fuller et al. 1980, 1982a, 1982b). Some rates are revised with experimental rates (see details in Koike et al. 1999). Our network includes 1988 nuclides from neutron and proton up to ^{209}Bi , presented in Table 1. The network is solved implicitly with an inverter of a sparse matrix (Timmes 1999).

2.3. Possible Progenitors for P-Process Nucleosynthesis inside SSADs

As the case of Type II supernovae, synthesis of p-nuclei inside SSADs requires the s-process seeds. The fallback after a supernova explosion is likely to be induced by deep gravitational potential of relatively massive stars and/or reverse shock inwardly propagating from the outer composition interfaces (Colgate 1971; Chevalier 1989; WW95). A total amount of fallback material increases as mass of a progenitor are enhanced (WW95; Fryer 1999, hereafter F99; Fryer & Heger 2000); Massive fallback is likely to take place for the progenitors with $M_{MS} \gtrsim 20M_{\odot}$ due to their large binding energy of the iron core, where M_{MS} is the mass of the progenitor on the main-sequence. For massive stars with $M_{MS} \gtrsim 40M_{\odot}$, supernova explosion cannot take place and collapsed matter forms a black hole promptly (F99). Several seconds after the core collapse a quasi-steady accretion disk is formed around the hole if the progenitor has sufficient angular momentum (MacFadyen & Woosley 1999), which is in a reasonable range of a progenitor model of Heger, Langer & Woosley (2000). Highly variable supercritical accretion with $0.01\text{--}0.1 M_{\odot} \text{ s}^{-1}$ is maintained for approximately 10–20 s (MacFadyen & Woosley 1999). For such high accretion rates, however, the accretion disk has enough high temperature ($\gtrsim 10^{10}$ K) for accreting gas to contain only protons and neutrons (Popham, Fryer & Woosley 1999). Therefore, the progenitors with $M_{MS} \gtrsim 40M_{\odot}$ is irrelevant for p-process nucleosynthesis inside SSADs.

While for progenitors with $M_{MS} = 20\text{--}40M_{\odot}$ a neutron star is formed soon after the core collapse. Supernova launches outward-going shock successfully but some fraction of supernova ejecta falls back onto the nascent neutron star, which is transformed to a black hole via massive fallback (F99). The accreting matter onto the

¹ The REACLIB compilation of reaction rates is available at: <ftp://quasar.physik.unibas.ch/pub/tommy/astro/reaclib/>

hole forms a disk with 10^{-4} – $10^{-2}M_{\odot} \text{ s}^{-1}$ lasting for hundreds to thousands of seconds (MacFadyen et al. 2001). After most of silicon layers of the progenitors has fallen back into the hole, the accretion rate is declined as $t^{-5/3}$ (Chevalier 1989; MacFadyen et al. 2001) and compositions of the accreting matter are those of explosively burned oxygen/neon layers via supernova shock. In a $20M_{\odot}$ progenitor model (Hashimoto 1995), the position of r_{out} ($=3000r_{\text{g}}$) is far from the core and located at $M_r \simeq 2.1M_{\odot}$, or the oxygen/neon layer, where the peak temperature during the shock propagation is too low to proceed appreciable nuclear burning of s-process seeds ($\lesssim 2 \times 10^9$ K). The material still leaves the s-process seeds even after the supernova explosion. Appreciable amounts of the seeds can fall back onto the compact object through the accretion disk. Accordingly, p-process nucleosynthesis operates inside a supercritical accretion disk driven by supernova explosion of the progenitors with $M_{\text{MS}} = 20$ – $40M_{\odot}$.

2.4. Initial Abundances of Fallback Matter

Chemical composition of fallback matter depends on masses of progenitors and fallback mechanisms. Because p-process nucleosynthesis inside SSADs needs s-process seeds, we set the compositions of the accreting gas at r_{out} to be averaged compositions of oxygen/neon layers of the progenitors of 10, 20, 30, and $40 M_{\odot}$, whose models are referred to as M10, M20, M30, and M40, respectively. These abundances were calculated with a network which contains 440 nuclei up to Bi. (Prantzos, Hashimoto & Nomoto 1990a). Although the progenitors with masses of $M_{\text{MS}} < 20M_{\odot}$ are unlikely to be relevant for p-process inside a SSAD, we also calculate abundances of p-nuclei for M10 because the abundance pattern is different from the others (Figure 1). It should be emphasized that these abundances were also adopted as the seed abundances in the p-process models of Rayet et al. (1990, 1995). Figure 1 shows the initial abundances of M10, M20, and M40, which are denoted by the dashed, solid, and thick-solid lines, respectively. The initial abundances of M30 are in between those of M20 and M40. The solar abundances are also depicted with the filled circles (Anders & Grevesse 1989).

Compositions of fallback matter are not those of the oxygen/neon layers of the progenitors but those of explosively burned layers because of supernova shock heating. Abundances of p-nuclei produced inside SSADs depend on amounts of s-process seeds, as we can see later. The explosively burned layers where the peak temperature of a shock wave is lower than 2×10^9 K still contain comparable s-process seeds to those before the explosion. Accordingly, the initial compositions of the oxygen/neon layers of the progenitors are relevant for our p-process model inside SSADs at least for fallback of the layers with relatively low peak temperature $\leq 2 \times 10^9$ K.

The compositions of fallback material discussed above are possibly altered when large-scale matter mixing is significant in supernova explosion. Such mixing is probably associated with fallback. Hence, we shall discuss effects of matter mixing on p-process nucleosynthesis in §3.3.

3. NUCLEOSYNTHESIS INSIDE SSADS

3.1. Abundance Distributions of P-Nuclei inside SSADs

As fallback material accretes onto a central object, temperature and density of the gas increase (see equations (1) and (2)) and thus abundances of the accreting gas are changed through a sequence of nuclear reactions from an initial composition described in §2.4. Using the nuclear reaction network and the self-similar solution, we can follow the evolution of the chemical composition inside SSADs during the infall toward the compact object through post-processing calculations for M10, M20, M30, and M40. The calculations are carried out from r_{out} to r_{in} . It should be noted that the nuclear energy generation is assumed to be much smaller than the viscous heating.

For disks with $\dot{m} \lesssim 10^5$, the maximum temperature of disks is less than 2×10^9 K which is the minimum temperature for the p-process to proceed in the so called *p-process layers* (PPLs) in Type II supernovae (Rayet et al. 1990, 1995). Therefore, p-process nucleosynthesis does not operate in the disks for such low accretion rates. For higher accretion rates, the accreting gas has higher temperature and the p-process can proceed significantly. The abundance distributions of p-nuclei are similar for the disks with various accretion rates, while the production site of p-nuclei shifts toward the outer part of the disk as the accretion rates increase. Thus, we show the results of $\dot{m} = 10^8$ as a representative case.

Figure 2 shows the abundance profiles, normalized with the solar abundances, of representative p-nuclei for M20. The abscissa is the radius of the fallback disk in units of r_{g} . The solid, thick-solid, dashed, thick-dashed, dotted, and thick-dotted lines indicate the abundances of ^{74}Se , ^{92}Mo , ^{138}La , ^{152}Gd , ^{180}Ta , and ^{196}Hg , respectively. At $r > 100 r_{\text{g}}$, temperatures of the accreting gas are too low to proceed appreciable synthesis of p-nuclei. The abundances of ^{152}Gd and ^{180}Ta are the same as the initial values. At $r \simeq 100 r_{\text{g}}$ ($T \simeq 1.3 \times 10^9$ K), ^{180}Ta increases via neutron capture of ^{179}Ta , contained in the fallback material initially. As the gas moves to the inner part of the disk, the temperature increases and the heavy p-nuclei ($A \geq 150$), such as ^{152}Gd , ^{180}Ta , and ^{196}Hg are rapidly destroyed through (γ, n) reactions. At $r \lesssim 50 r_{\text{g}}$ ($T \gtrsim 2.0 \times 10^9$ K), however, these isotopes are drastically produced. This is due to the photodisintegrations of the neutron-rich seed elements when the temperature of the accreting gas attains to $2 - 3 \times 10^9$ K comparable to PPLs (Rayet et al. 1995). Thus, the p-processes operate efficiently inside the accretion disk as in the PPLs. The intermediate p-nuclei ($100 \leq A < 150$) also enhance via the p-process. It should be noted that $t_{\text{dr}} \simeq 0.1$ – 1 s in this region is comparable to the time-scale of shock propagation through PPLs (Rayet et al. 1995).

For a region $r \lesssim 30r_{\text{g}}$ ($T \gtrsim 2.8 \times 10^9$ K), (γ, p) and (γ, α) reactions of the heavy and intermediate isotopes dominate over (γ, n) reactions; while for the light p-nuclei ($A < 100$), such as ^{74}Se and ^{92}Mo , (γ, n) reactions are still dominant processes. The light p-nuclei are eventually depleted via (γ, p) and (γ, α) reactions near $20 r_{\text{g}}$ ($T \sim 3.6 \times 10^9$ K). It is noted that the abundance profiles for all models are similar, while the more p-nuclei are produced the more massive are progenitors because of the richness of s-process seeds (Figure 1).

3.2. Ejected Masses of P-Nuclei from SSADs

Many astrophysical objects involving an accretion disk are observed to produce jets and/or winds (e.g., Livio 1999 and references therein). Hence, as the accreting gas falls back onto the central object, some fraction of gas is possibly ejected from the disk via jets and/or winds. The processed material ranging from r_{in} to r_{ej} is supposed to be ejected. Then we can estimate the averaged mass fraction \bar{X}_i of the i -th p-nucleus ejected from the disks,

$$\bar{X}_i = \frac{2\pi}{M(r_{\text{ej}})} \int_{r_{\text{in}}}^{r_{\text{ej}}} X_i(r) \Sigma(r) r dr, \quad (4)$$

where $\Sigma(r)$ is the column density of the disk. Here $M(r_{\text{ej}})$ is the mass of the disk from r_{in} to r_{ej} and the fraction of the ejected gas to the accreting gas is assumed to be constant in radius. To compare the p-nuclei abundances ejected from the fallback disks with the solar abundances, we calculate the overproduction factors (OPFs) F_i of 35 p-nuclei (Rayet et al. 1995):

$$F_i = (\bar{X}_i / X_{i,\odot}) / F_0, \quad (5)$$

where $X_{i,\odot}$ is the mass fraction in the solar system and $F_0 = \sum_{i=1}^{35} (\bar{X}_i / X_{i,\odot}) / 35$. In many accretion powered systems, matter ejection via jets and/or winds could be originated from the inner region of the accretion disks. Therefore, we set r_{ej} to be $100r_g$ (Junor et al. 1999). The chemical composition of the ejected material is assumed to be constant throughout a jet and/or a wind. Abundances of p-nuclei increase due to β -decays of their unstable parent nuclei after the freeze out. However, abundances of most p-nuclei are not appreciably enhanced after the β -decays (see §4.2).

Figures 3 and 4 show the OPFs of 35 p-nuclei for M20 and M10, respectively. It is emphasized that the abundance profiles have similar features to those in Type II supernovae (Rayet et al. 1995). The light p-nuclei, $^{92,94}\text{Mo}$ and $^{96,98}\text{Ru}$ are underproduced in our calculations. This is due to the deficiency of their s-process seeds (Fuller & Meyer 1995). The intermediate mass p-nuclei, ^{113}In , ^{115}Sn , and ^{138}La , cannot be produced appreciably for M10 and M20. It is noted that ^{113}In and ^{115}Sn are largely enhanced through β -decays after ejection via jets and/or winds (see §4.2). ^{152}Gd is underproduced in our calculations, while a large amount of ^{152}Gd is synthesized in the stellar s-process (Prantzos et al. 1990a). ^{164}Er is also underproduced in our calculations. The overproductions of ^{74}Se (M20) and ^{184}Os (M10) are attributed to the ample-ness of their s-process seeds. The OPF of ^{120}Te is largely increased for M10 compared with that of M20. The OPFs of Se, Kr, and Sr for M10 are smaller than those for M20 but those of p-nuclei with $A \geq 168$ are larger. Such profiles of the OPFs are also responsible for initial abundance distributions of s-process seeds. The OPFs for M30 and M40 are similar profiles to those for M20. However, F_0 for M30 and M40 are larger than F_0 for M20 (Table 2). This is because more massive progenitor has larger amounts of s-process seeds (Figure 1).

Profiles of the OPFs ejected from SSADs depend on initial abundance distributions of s-process seeds. The s-process seeds are mainly synthesized during a helium core burning stage in massive stars. The s-process nucleosynthesis in massive stars has been extensively investigated by many authors (e.g., Prantzos et al. 1990a; Käppeler et al. 1994; Rayet & Hashimoto 2000); Uncertainties in some

key nuclear reactions still preclude precise estimation of s-process yields.

3.3. Proton and Helium Contamination through Matter Mixing

Several observations in SN 1987A support the occurrence of large-scale mixing in the ejecta. Newly synthesized ^{56}Ni near the collapsed core is likely to be mixed up into the hydrogen envelope as indicated from observations in early phase; X-ray and γ -ray light curves (e.g., Kumagai et al. 1989 and references therein) and optical spectroscopy (e.g., Mitchell et al. 2001 and references therein). Two-dimensional simulations of supernova explosions (Müller, Fryxell & Arnett 1991; Herant & Benz 1992; Nagataki, Shimizu & Sato 1998) indicate that the large-scale mixing is caused via Rayleigh-Taylor instability. A recent high-resolution simulation by Kifonidis et al. (2000) shows that a large amount of ^4He is mixed down near the iron core by the Rayleigh-Taylor instability. Hydrogen is also shown to be mixed down to the core (Hachisu et al. 1990). Moreover, several analyses of observations in SN 1987A are also preferable to mixing of the outer hydrogen-rich envelope down to the inner metal-rich core; the width of plateau-like peak of the bolometric light curves (Shigeyama & Nomoto 1990), line profiles in late spectral evolution (Kozma & Fransson 1998), and the light curve for the first 4 months (Blinnikov et al. 2000). Thus, appreciable amounts of proton and helium are likely to be mixed down to the inner core via the Rayleigh-Taylor instability in SN 1987A. Certain fractions of proton and helium are accordingly mixed into the oxygen/neon layers.

Such mixing is probably generic in core-collapsed supernovae; recent X-ray observations in Cas A (Douvion et al. 1999; Hughes et al. 2000), emission line profiles of SN 1988A (Spyromilio 1991) and SN 1993J (Spyromilio 1994), and optical and infrared spectroscopies of SN 1995V (Fassia et al. 1998) and SN 1998S (Fassia et al. 2001).

Moreover, recent investigation for anomalous composition in a companion of the black hole binary Nova Sco suggests that the companion is polluted by material ejected in the supernova accompanied with the formation of the hole (Israelian et al. 1999). The progenitor in this system is likely to experience substantial fallback (\simeq a few M_{\odot}) and matter mixing in supernova ejecta (Podsiadlowski et al. 2002). Such fallback with mixing is also preferable to the large abundance of Zn observed in the very metal-poor stars (Umeda & Nomoto 2002). Therefore, the fallback gas is expected to be contaminated with some fractions of proton and helium via the large-scale mixing.

To investigate effects of proton and helium contamination of the fallback material on the p-process nucleosynthesis, we add an arbitrary fraction of proton or helium to the initial abundance of M20 and calculate the abundance distributions inside SSADs. The initial proton abundance of the fallback matter highly depends on large-scale mixing and fallback mechanism. There exists no reliable estimation of the initial proton abundance. Analyses of observations in SN 1987A indicate that the mass fraction of proton is 0.01 (Blinnikov et al. 2000) or up to 0.3 (Shigeyama & Nomoto 1990). Hence we examine the cases of the initial mass fraction of proton $X_p = 0.01, 0.1,$ and 0.3 , which are referred as models M20P001, M20P01, and M20P03, re-

spectively. In these models, p-nuclei are produced via not only photodisintegration of s-process seeds but radiative proton capture of lighter nuclei.

Figure 5 shows the OPFs for M20P001 with $\dot{m} = 10^8$. The most remarkable is an enhancement of ^{92}Mo . Even if the fallback material contains a small fraction of proton, radiative proton captures as well as photodisintegrations are efficient. The light p-nuclei, ^{74}Se , ^{78}Kr , and ^{84}Sr , are increased, while the light p-nuclei underproduced in M20, such as ^{94}Mo , ^{96}Ru , and ^{98}Ru , are still deficient. The intermediate mass p-nuclei, ^{114}Sn , ^{115}Sn , and ^{138}La are underproduced as M20. The OPFs of the heavy p-nuclei are decreased compared with M20 though abundances of these p-nuclei are not appreciably changed. This is because the averaged OPF, F_0 , is increased (equation (5)). We also find that profiles of the OPFs weakly depend on X_p for $\dot{m} = 10^8$: the OPFs for M20P01 and M20P03 are not significantly changed from those for M20P001. The averaged OPFs, F_0 , of M20P001, M20P01, and M20P03 are larger than that of M20 and listed in Table 2. For models with initial abundances of M10, M30, and M40 added by proton of $X_p = 0.01, 0.1, \text{ and } 0.3$, the OPFs are similar profiles to model with the initial abundance of $20M_\odot$ model added by the same fraction of proton (i.e., same X_p) though the averaged OPFs, F_0 , are significantly increased for models with massive progenitor (Table 2).

For $\dot{m} = 10^6$, the profiles of the OPFs change as protons are injected. Appreciable amounts of the p-nuclei which are deficient in model M20 are produced in SSADs. For $X_p = 0.01$ (M20P001), ^{92}Mo and ^{138}La are overproduced. The overproductions of ^{92}Mo and ^{138}La are more prominent in M20P01 (Figure 6) compared with M20P001. When $X_p = 0.3$ (model M20P03; Figure 7), ^{96}Ru , ^{113}Sn , and ^{114}Sn become abundant because of very efficient proton captures. However, the overall profile of the OPFs becomes worse compared with the solar one. F_0 drastically increases compared with the cases of small proton inclusion; F_0 are equal to 67.68, 41.84, and 2882, for M20P001, M20P01, and M20P03, respectively. It should be noted that ^{94}Mo , ^{98}Ru , and ^{115}Sn are underproduced even if protons exist abundantly.

Concerning helium contamination of fallback material via large-scale mixing, the OPFs are not appreciably changed from those of M20 even if a significant fraction of ^4He , up to 0.5, is added to the initial abundance of M20. Hence, amounts of p-nuclei produced inside SSADs are independent of an amount of ^4He included in fallback material, while α elements, such as ^{44}Ti , are enhanced.

4. DISCUSSION

4.1. Contribution of SSADs to Chemical Evolution of P-Nuclei

We discuss contribution from SSADs to chemical evolution of p-nuclei to estimate relative contribution from SSADs in respect to supernovae. In this aim we average the overproduction factor F_0 of p-nuclei produced by supernovae or SSADs using the initial mass function (IMF) $\xi(M)$. The IMF-weighted OPF is calculated as

$$\langle F_0 \rangle_{\text{IMF}} = \frac{\int_{M_l}^{M_u} F_0(M) M_{\text{cont}}(M) \xi(M) dM}{\int_{M_l}^{M_u} \xi(M) dM} \quad (6)$$

where M_l and M_u are the lower and upper mass limits of progenitors and M_{cont} is the total mass (in units of M_\odot) which contributes to the production of p-nuclei via supernovae or SSADs.

We assume that the progenitors of $13 \leq M_{\text{MS}}/M_\odot \leq 20$ can produce p-nuclei via supernova explosion (Rayet et al. 1995), while the progenitor with $20 \leq M_{\text{MS}}/M_\odot \leq 40$ can yield p-nuclei through SSADs driven by massive fallback. For supernovae and SSADs, M_{cont} is the mass of the PPLs, M_{PPL} (Rayet et al. 1995) and the ejected mass from a disk via jets and/or winds, M_{ej} , respectively. Adopting $\xi(M) \propto M^{-2.3}$ proposed by Salpeter (1955), we can calculate $\langle F_0 \rangle_{\text{IMF}}$ as 18.3 for supernovae. Here we use the results of Rayet et al. (1995) for M_{PPL} and $F_0(M)$ (in their Tables 2 and 3). A calculation is performed in a similar manner to Rayet et al. (1995).

Next we estimate $\langle F_0 \rangle_{\text{IMF}}$ for SSADs for the two cases: no proton mixing and complete mixing. In actual situations, uncertain fractions of fallback matter are affected by matter mixing. Hence $\langle F_0 \rangle_{\text{IMF}}$ for SSADs is located between the two estimations. Firstly we discuss the case in absence of matter mixing and then those with complete mixing.

4.1.1. The Case in The Absence of Matter Mixing

To calculate $\langle F_0 \rangle_{\text{IMF}}$ for SSADs, we need an estimation of the total fallback mass with s-process seeds, M_{seed} . An amount of fallback material has been estimated by WW95 and F99 through numerical simulations of core collapse and supernova explosion. Amounts of fallback material M_f are presented in Table 3 for the fallback models of WW95 and F99. To operate the p-process in SSADs, fallback material should contain the s-process seeds. Accordingly, to calculate M_{seed} , besides the amount of fallback matter, both the abundance distribution of the progenitor and the peak temperature of the supernova shock are needed. In Table 3, we also show the mass coordinate of the base of oxygen burning layers, M_{Ob} and the mass coordinate where the peak temperature is 2×10^9 K, M_{dest} for the progenitor and explosion models with masses of 15, 20, 25, and $40 M_\odot$ (Hashimoto 1995). All s-process seeds are assumed to be destroyed in the region of the mass coordinate $M_r \leq M_{\text{dest}}$ and thus disk p-process can operate only for fallback material with $M_r > M_{\text{dest}}$. Hence we can estimate M_{seed} , which are also presented in Table 3, for WW95 and F99. For the fallback model of WW95, $M_{\text{seed}}(30M_\odot)$ is estimated as $2.41M_\odot$ provided that M_{dest} for the $30M_\odot$ progenitor is equal to that of the $25M_\odot$ progenitor. For the fallback model of F99, we set simply $M_{\text{seed}}(20M_\odot) = 0.5[M_{\text{seed}}(15M_\odot) + M_{\text{seed}}(25M_\odot)]$ and $M_{\text{seed}}(30M_\odot) = \frac{1}{3}[2M_{\text{seed}}(25M_\odot) + M_{\text{seed}}(40M_\odot)]$.

Moreover, some fractions of synthesized p-nuclei inside SSADs are ejected from the disks via jets and/or winds as in many objects associated with an accretion disk (e.g., Livio 1999). We assume that the ratio ϵ of the mass ejection rate \dot{M}_{ej} to the mass accretion rate is constant in time, or $\dot{M}_{\text{ej}} = \epsilon \dot{M}$. Hence the total ejected mass is also expressed as $M_{\text{ej}} = \epsilon M_{\text{seed}}$. The ratio ϵ are 0.001–0.01 (Eggum, Coroniti & Katz 1988) and 0.03–0.1 (Kudoh, Matsumoto & Shibata 1998) estimated from numerical simulations of jets originated from an accretion disk. However, ϵ may be larger as suggested by observations in

X-ray binaries; SS433 (Kotani 1997) and GRS 1915+105 (Fender & Pooley 2000; Belloni et al. 2000).

Using the calculated values of F_0 for our SSAD models (Table 2), we evaluate $\langle F_0 \rangle_{\text{IMF}}$ as 1.640 $\epsilon_{0.01}$ and 2.864 $\epsilon_{0.01}$ with the estimation of amounts of fallback matter of WW95 and F99, respectively, where $\epsilon_{0.01} = \epsilon/0.01$. Thus $\langle F_0 \rangle_{\text{IMF}}$ for SSADs are smaller than that for supernovae (= 18.30) unless ϵ is as large as 0.1. It should be noted that $\langle F_0 \rangle_{\text{IMF}}$ slightly decreases for a steep IMF slope with $\xi(M) \propto M^{-2.7}$ (e.g., Kroupa 2002) and also reduce by 30–50% if $M_u = 30M_\odot$.

4.1.2. The Case with Complete Matter Mixing

We proceed the case of fallback with complete proton mixing. We assume matter contains proton of $X_p = 0.01$ throughout fallback. The proton mixing needs the hydrogen envelope of progenitors, which is decreased due to mass loss for massive progenitors (e.g., Chiosi & Maeder 1986). The upper limit M_u possibly decreases for cases with proton mixing and are taken to be $M_u = 35M_\odot$ (Fryer & Kalogera 2001). As in the absence of matter mixing, we calculate $\langle F_0 \rangle_{\text{IMF}}$ as 5.027 $\epsilon_{0.01}$ and 9.583 $\epsilon_{0.01}$ for the fallback models of WW95 and F99, respectively. Here we set $F_0(35M_\odot) = 0.5[F_0(30M_\odot) + F_0(40M_\odot)]$. The enhancement of $\langle F_0 \rangle_{\text{IMF}}$ compared with no proton mixing is responsible for the increase in F_0 for the models with proton mixing (Table 2). Hence, in the case with complete mixing, the SSADs-origin p-nuclei are likely to comparably contribute to the chemical evolution of p-nuclei as the supernovae-origin p-nuclei.

In particular, SSADs probably have significant contribution to the ^{92}Mo evolution. Overproduction of ^{92}Mo takes place for any \dot{m} (Figures 5–7). Accordingly, the overproduction is realized inside SSADs throughout the duration in which a large fraction of fallback matter accretes onto a central compact object. Even for the cases of small X_p , ^{92}Mo is overproduced inside SSADs; This is the case of $X_p \gtrsim 0.005$. Thus, contribution to the ^{92}Mo evolution is considerable for a small amount of proton $\sim 0.01M_\odot$ mixed into the fallback matter of 0.1 to several M_\odot .

On the other hand, ^{96}Ru and ^{138}La are overproduced only for the case of $\dot{m} = 10^6$. The accretion rate of fallback matter is declined to relatively small accretion rates $\dot{m} \sim 10^6$ at several months after the explosion (Mineshige et al. 1997) and large amounts of fallback matter have already accreted onto a central remnant. Therefore, only a small amount of fallback matter are processed inside SSADs, which are enable to overproduce ^{96}Ru and ^{138}La .

4.2. Abundance Change of P-Nuclei through Jets and Winds

In SSADs, p-nuclei are mainly produced in the region 20–70 r_g for $\dot{m} = 10^8$ (Figure 2) where an accreting gas is mainly ejected via winds. Parent nuclei which decay into p-nuclei through β -decays are also expelled via winds and thus enhance amounts of p-nuclei. Taking into account the β -decays after freeze out, we estimate abundances of p-nuclei ejected from a SSAD. We find that p-nuclei other than ^{92}Mo , ^{94}Mo , ^{113}In , and ^{115}Sn are not appreciably increased via β -decays of their parent nuclei; Their ratio after to before β -decays are 1.100, 1.215, 13.77, and 18.33, respectively, for M20. Here all the parent nuclei has been

assumed to decay to their daughter p-nuclei. When proton is abundantly mixed into fallback material, the abundances of ^{92}Mo and ^{94}Mo are not significantly changed but ^{113}In and ^{115}Sn are largely enhanced. For M20P03 ($X_p = 0.3$), the ratio of the abundances of ^{113}In , and ^{115}Sn after to before β -decays become 9.797 and 42.41, respectively. However, the averaged OPFs, F_0 , are not appreciably changed because of small OPFs of ^{113}In and ^{115}Sn up to ~ 0.07 before β -decays (Figures 3–7). Thus, β -decays after freeze out has only minor effect on estimation of $\langle F_0 \rangle_{\text{IMF}}$ discussed in §4.1.

4.3. Neutron Star Kick

If a compact object breaks out a supernova remnant, matter fallback onto the object ceases. Many observations reveal that pulsars have larger space velocities (200–1000 km s^{-1}) than those of their progenitor (e.g., Lai et al. 2001 and references therein). Such high velocities are invoked to kicks of nascent neutron stars via asymmetric supernova explosions. The supercritical accretion ($\dot{m} > 10^5$) investigated in the present paper is realized until about 4 years after an explosion (Mineshige et al. 1997). The expansion velocity of the supernova remnant is much larger than the typical kick velocity of pulsars. The material therefore continues to fall back during the supercritical accretion of our interest. However, the later expansion of the remnant is decelerated by ambient material from progenitor winds. The pulsar eventually breaks through the supernova remnant and matter fallback onto it ceases.

5. CONCLUDING REMARKS

We have investigated the p-process nucleosynthesis inside SSADs around a compact object of $1.4M_\odot$. Supernova explosion of 20–40 M_\odot progenitors is probably responsible for the p-process nucleosynthesis inside SSADs. The chemical compositions of the accreting gas far from the central object have been assumed to be those of the oxygen/neon layers of the progenitor in the model of 10, 20, 30, and 40 M_\odot stars. It is found that when $\dot{m} > 10^5$ the temperature of the accreting gas attains to $2 - 3 \times 10^9$ K and appreciable nuclear reactions take place to produce the p-nuclei. We have also estimated the OPFs of the p-nuclei in the ejected material from the accretion disks via jets and/or winds to compare the abundances of the ejected matter with the solar abundances. The resultant p-nuclei profiles have similar features to those for Type II supernovae (Rayet et al. 1995). The light and intermediate mass p-nuclei such as ^{92}Mo , ^{94}Mo , ^{96}Ru , ^{98}Ru , ^{114}Sn , and ^{138}La are underproduced. The amounts of p-nuclei and profiles of the OPFs ejected from SSADs depend on initial abundance distributions of s-process seeds.

Moreover, for investigating the effects of proton and helium contamination via large-scale mixing in a supernova explosion of fallback material on the p-process nucleosynthesis, we have added some fractions of proton or helium to the initial composition for the cases of 10, 20, 30, and 40 M_\odot progenitors and calculated the OPFs of the p-nuclei in the ejected material. It has been found that significant fractions of ^4He inclusion cause small changes in the OPFs. Even for a small amount of proton included in fallback material, p-nuclei are synthesized through not only photodisintegrations but radiative proton captures. The most

prominent is an enhancement of ^{92}Mo . ^{138}La is also overproduced for $\dot{m} = 10^6$. If fallback matter includes abundant proton, appreciable amounts of the p-nuclei, such as ^{92}Mo , ^{96}Ru , ^{113}Sn , and ^{114}Sn , which are deficient in Type II supernovae, can be produced for $\dot{m} = 10^6$, though the overall profiles of the OPFs becomes worse compared with the solar ones.

We have discussed the contribution from the p-process nucleosynthesis in SSADs to galactic chemical evolution of p-nuclei. We conclude that p-process in SSADs comparably contributes to chemical evolution of p-nuclei as in supernovae if several percents of fallback matter are ejected from SSADs. In particular the p-process in SSADs may be important for the chemical evolution of ^{92}Mo and possibly compensates the underproduction in Type II supernovae. Contribution from SSADs to the chemical evolution of ^{96}Ru and ^{138}La is unlikely to be significant.

Numerical simulations of supernova-driven jets present

the peculiar nucleosynthesis of the alpha-rich freeze out (Nagataki et al. 1997): The p-process will be affected by jets as SN1987A. Some gamma-ray bursts are likely to be caused by aspherical jet-induced supernova explosions (MacFadyen & Woosley 1999; MacFadyen et al. 2001). Numerical calculations indicate that in such explosions a SSAD is formed around a new-born compact object and a substantial amount of fallback ($\simeq 0.2M_{\odot}$) followed by mixing takes place (Fryer & Heger 2000; Höflich, Khokhlov & Wang 2001). Hence some gamma-ray bursts possibly accompany with the synthesis of p-nuclei; Our SSAD p-process model would be responsible for the synthesis of p-nuclei in these bursts.

We are grateful to Dr. Takashi Yoshida for his helpful processing nuclear data and useful discussion. We also thank the anonymous referee for useful comments.

REFERENCES

- Anders, E., & Grevesse, N. 1989, *Geochim. Cosmochim. Acta*, 53, 197
- Arnould, M. 1976, *A&A*, 46, 117
- Arnould, M., Rayet, M., Hashimoto, M. 1998, in *Tours Symposium on Nuclear Physics III*, ed. M. Arnould et al. (New York: AIP), 626
- Audi, G., & Wapstra, A. H. 1995, *Nucl. Phys. A*, 595, 409
- Belloni, T., Migliari, S., & Fender, R. P. 2000, *A&A*, 358, L29
- Blinnikov, S., Lundqvist, P., Bartunov, O., Nomoto, K., & Iwamoto, K. 2000, *ApJ*, 532, 1132
- Chevalier, R. A. 1989, *ApJ*, 346, 847
- Chiosi, C., Maeder, A. 1986, *ARA&A*, 24, 329.
- Colgate, S. A. 1971, *ApJ*, 163, 221
- Costa, V., Rayet, M., Zappalà, R. A., & Arnould, M. 2000, *A&A*, 358, 67
- Douvion, T., Lagage, P. O., & Cesarsky, C. J. 1999, *A&A*, 352, L111
- Eggum, G. E., Coroniti, F. V., & Katz, J. I. 1988, *ApJ*, 330, 142
- Fassia, A., Meikle, W. P. S., Geballe, T. R., Walton, N. A., Pollacco, D. L., Rutten, R. G. M., & Tinney, C. 1998, *MNRAS*, 299, 150
- Fassia, A., et al. 2001, *MNRAS*, 325, 907
- Fender, R. P., & Pooley, G. G. 2000, *MNRAS*, 318, L1
- Fryer, C. L. 1999, *ApJ*, 522, 413
- Fryer, C. L., Colgate, S. A., & Pinto, P. A. 1999, *ApJ*, 511, 885
- Fryer, C. L., & Heger, A. 2000, *ApJ*, 541, 1033
- Fryer, C. L., Kalogera, V. 2001, *ApJ*, 554, 548
- Fujimoto, S., Arai, K., Matsuba, R., Hashimoto, M., Koike, O., & Mineshige, S. 2001, *PASJ*, 53, 509
- Fuller, G. M., Fowler, W. A., & Newman, M. J. 1980, *ApJS*, 42, 447
- . 1982a, *ApJS*, 48, 279
- . 1982b, *ApJ*, 252, 715
- Fuller, G. M., & Meyer, B. S. 1995, *ApJ*, 453, 792
- Goriely, S., Arnould, M., Borzov, I., & Rayet, M. 2001, *A&A*, 375, 35
- Goriely, S., Jose, J., Hernanz, M., Rayet, M., & Arnould, M. 2002, *A&A*, 383, L27
- Hachisu, I., Matsuda, T., Nomoto, K., & Shigeyama, T. 1990, *ApJ*, 358, L57
- Hashimoto, M. 1995, *Prog. Theor. Phys.*, 94, 663
- Hashimoto, M., Arai, K. 1985, *Phys. Rep. Kumamoto Univ.*, 7, 1
- Heger, A., Langer, N., & Woosley, S. E. 2000, *ApJ*, 528, 368
- Herant, M., & Benz, W. 1992, *ApJ*, 387, 294
- Hoffman, R. D., Woosley, S. E., Fuller, G. M., & Meyer, B. S. 1996, *ApJ*, 460, 478
- Horiguchi, T., Tachibana, T., & Katakura, J. 1996, *Chart of The Nuclides*, Nuclear Data Center, Japan Atomic Energy Research Institute, Ibaraki
- Howard, W. M., Meyer, B. S., Woosley, S. E. 1991, *ApJ*, 373, L5
- Hawley, J. F. 2000, *ApJ*, 528, 462
- Höflich, P., Khokhlov, A., & Wang, L. 2001, in *20th Texas Symposium on Relativistic Astrophysics*, ed. J. C. Wheeler & H. Martel (New York:AIP), 459
- Hughes, J. P., Rakowski, C. E., Burrows, D. N., & Slane, P. O. 2000, *ApJ*, 528, L109
- Israerian, G., Rebollo, R., Basrl, G., Casares, J., & Martin, E. L. 1999, *Nature*, 401, 142
- Jaeger, M., Kunz, R., Mayer, A., Hammer, J.W., Staudt, G., Kratz, K.-L., & Pfeiffer, B. 2001, *Phys. Rev. Lett.*, 87, 202501
- Junor, W., Biretta, J. A., & Livio, M. 1999, *Nature*, 401, 891
- Käppeler, F., et al. 1994, *ApJ*, 437, 396
- Kifonidis, K., Plewa, T., Janka, H.-Th., & Müller, E. 2000, *ApJ*, 531, L123
- Koike, O., Hashimoto, M., Arai, K., & Wanajo, S. 1999, *A&A*, 342, 464
- Kotani, T. 1997, PhD thesis, The University Tokyo
- Kudoh, T., Matsumoto, R., & Shibata, K. 1998, *ApJ*, 508, 186
- Kozma, C., & Fransson, C. 1998, *ApJ*, 497, 431
- Kroupa, P. 2002, *Science*, 295, 5552
- Kumagai, S., Shigeyama, T., Nomoto, K., Itoh, M., Nishimura, J., & Tsuruta, S. 1989, *ApJ*, 345, 412
- Lai, D., Chernoff, D. F., & Cordes, J. M. 2001, *ApJ*, 549, 1111
- Livio, M. 1999, *Phys. Rep.*, 311, 225
- MacFadyen, A. I., & Woosley, S. E. 1999, *ApJ*, 524, 262
- MacFadyen, A. I., Woosley, S. E., & Heger, A. 2001, *ApJ*, 550, 410
- Mineshige, S., Nomura, H., Hirose, M., Nomoto, K., & Suzuki, T. 1997, *ApJ*, 489, 227
- Mitchell, R. C., Baron, E., Branch, D., Lundqvist, P., Blinnikov, S., Hauschildt, P. H., & Pun, C. S. J. 2001, *ApJ*, 556, 979
- Müller, E., Fryxell, B., & Arnett, D. 1991, *A&A*, 251, 505
- Nagataki, S., Shimizu, T. M., & Sato, K. 1998, *ApJ*, 495, 413
- Nagataki, S., Hashimoto, M., Sato, K., Yamada, S. 1997, *ApJ*, 486, 1026
- Podsiadlowski, P., Nomoto, K., Maeda, K., Nakamura, T., Mazzali, P., & Schmidt, B. 2002, *ApJ*, 567, 491
- Popham, R., Woosley, S. E., & Fryer, C. 1999, *ApJ*, 518, 356
- Prantzos, N., Hashimoto, M., & Nomoto, K. 1990a, *A&A*, 234, 211
- Prantzos, N., Hashimoto, M., Rayet, M., & Arnould, M. 1990b, *A&A*, 238, 455
- Rauscher, T., & Thielemann, F.-K. 2000, *At. Data Nucl. Data Tables*, 75, 1
- . 2001, *At. Data Nucl. Data Tables*, 79, 47
- Rayet, M., Arnould, M., Hashimoto, M., Prantzos, N., & Nomoto, K. 1995, *A&A*, 298, 517
- Rayet, M., & Hashimoto, M. 2000, *A&A*, 354, 740
- Rayet, M., Prantzos, N., & Arnould, M. 1990, *A&A*, 227, 271
- Salpeter, E.E. 1955, *ApJ*, 121, 161
- Schatz, H., et al. 1998, *Phys. Rep.*, 294, 167
- Shigeyama, T., & Nomoto, K. 1990, *ApJ*, 360, 242
- Spyromilio, J. 1991, *MNRAS*, 253, 25
- . 1994, *MNRAS*, 266, 61
- Timmer, F. X. 1999, *ApJS*, 124, 241
- Umeda, H., & Nomoto, K. 2002, *ApJ*, 565, 385
- Woosley, S. E., & Howard, W. M. 1978, *ApJS*, 36, 285
- Woosley, S. E., Hartmann, D. H., Hoffman, R. D., & Haxton, W. C. 1990, *ApJ*, 356, 272
- Woosley, S. E., & Weaver, T. A. 1995, *ApJS*, 101, 181 (WW95)

TABLE 1
ELEMENTS INCLUDED IN THE NUCLEAR REACTION NETWORK.

elements	A	elements	elements	A
H	1– 3	Cu	56– 71	La 121–139
He	3– 6	Zn	57– 74	Ce 126–142
Li	6– 8	Ga	60– 77	Pr 127–143
Be	7– 10	Ge	66– 76	Nd 132–150
B	8– 12	As	70– 77	Pm 133–151
C	11– 14	Se	71– 82	Sm 136–154
N	12– 15	Br	74– 83	Eu 137–155
O	14– 20	Kr	75– 86	Gd 140–160
F	17– 22	Rb	78– 87	Tb 143–161
Ne	17– 24	Sr	80– 88	Dy 146–164
Na	20– 27	Y	82– 92	Ho 149–165
Mg	20– 29	Zr	84– 96	Er 151–170
Al	22– 31	Nb	86– 97	Tm 152–171
Si	24– 34	Mo	88–100	Yb 154–176
P	27– 38	Tc	90–101	Lu 156–177
S	28– 42	Ru	92–104	Hf 158–180
Cl	31– 45	Rh	94–105	Ta 164–181
Ar	32– 48	Pd	96–110	W 166–186
K	35– 49	Ag	98–111	Re 168–187
Ca	36– 50	Cd	100–116	Os 170–192
Sc	39– 51	In	103–117	Ir 172–193
Ti	40– 53	Sn	105–124	Pt 174–198
V	43– 55	Sb	106–125	Au 178–200
Cr	44– 58	Te	108–130	Hg 180–204
Mn	46– 64	I	114–131	Tl 186–205
Fe	47– 65	Xe	116–136	Pb 190–208
Co	50– 66	Cs	117–137	Bi 192–209
Ni	51– 68	Ba	120–138

TABLE 2
OVERPRODUCTION FACTOR F_0 EJECTED FROM SSADS FOR THE
PROGENITORS OF 10, 20, 30, AND 40 M_\odot AND FOR VARIOUS
VALUES OF PROTON CONTAMINATION X_p .

M_{MS} (M_\odot)	F_0^{a}			
	$X_p = 0$	$X_p = 0.01$	$X_p = 0.1$	$X_p = 0.3$
10	18.15	26.73	21.40	18.03
20	49.64	161.1	88.46	89.03
30	102.0	461.8	259.1	235.9
40	138.3	698.5	422.3	332.2

^aAll F_0 are calculated for the case of $\dot{m} = 10^8$.

TABLE 3
VARIOUS MASSES OF PROGENITORS AND FALLBACK MATTER

M_{MS}^{a}	M_{Ob}^{b}	$M_{\text{dest}}^{\text{c}}$	WW95 model			F99 model		
			M_{f}^{d}	$M_{\text{rem}}^{\text{e}}$	$M_{\text{seed}}^{\text{f}}$	M_{f}^{d}	$M_{\text{rem}}^{\text{e}}$	$M_{\text{seed}}^{\text{f}}$
15	1.37	1.55	0.11	1.43	0	0.2	1.52	0
20	1.67	1.8	0.32	2.06	0.26
25	1.48	1.8	0.29	2.07	0.27	3.8	5.58	2.0
30	2.41	4.24
40	2.36	3.5	8.36	10.34	4.84	10.3	11.01	6.8

Note. — All masses are in units of M_{\odot} .

^aProgenitor mass on the main-sequence.

^bLocation of the base of oxygen burning shell from Hashimoto (1995).

^cLocation where the peak temperature of supernova shock is equal to 2×10^9 K from Hashimoto (1995).

^dFallback mass.

^eRemnant mass after fallback.

^fEstimated fallback mass with s-process seeds for p-nuclei.

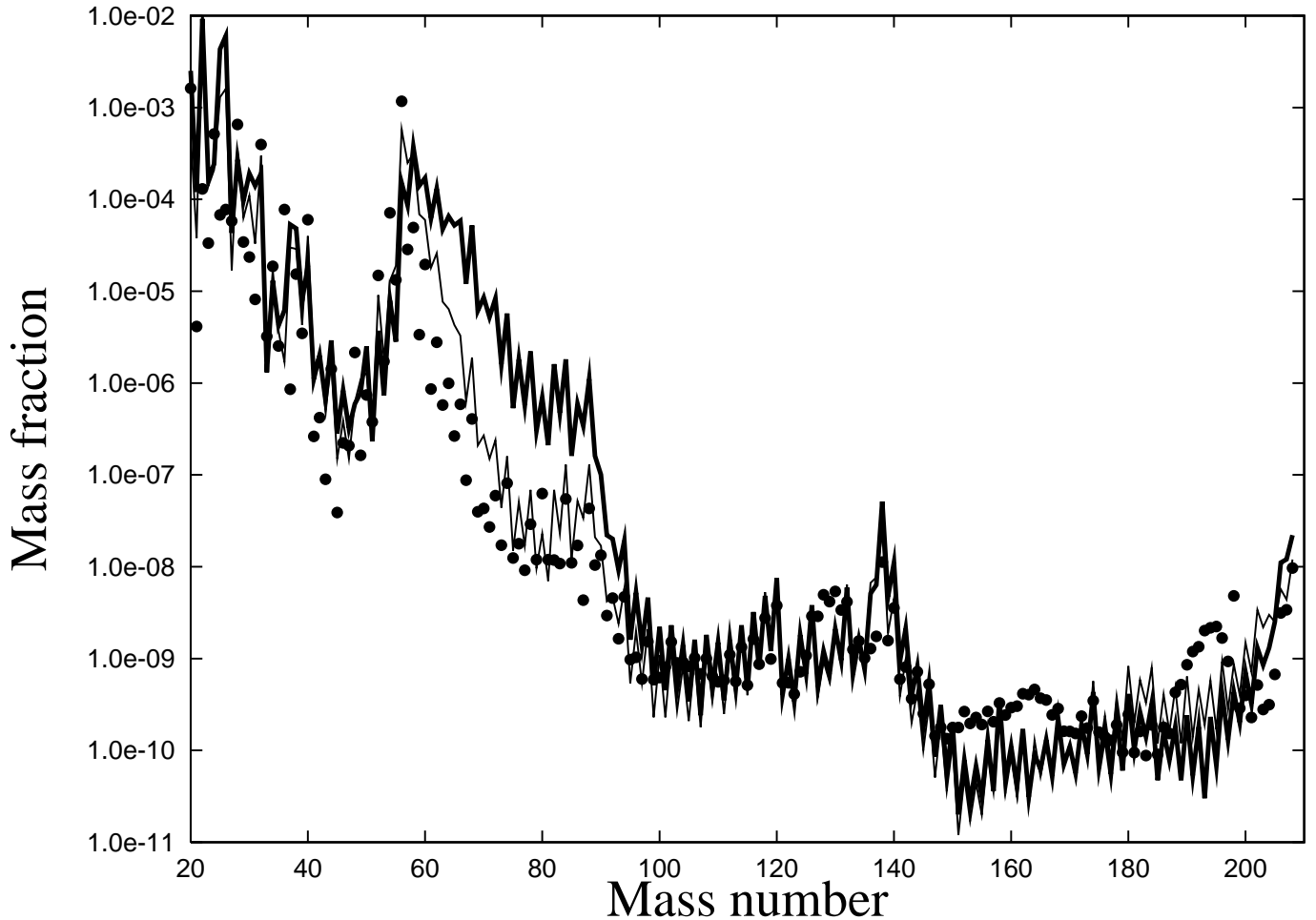


FIG. 1.— The initial abundances of models M10 (dashed line) M20 (solid line), and M40 (thick-solid line). The filled circles are the solar abundance (Anders & Grevesse 1989).

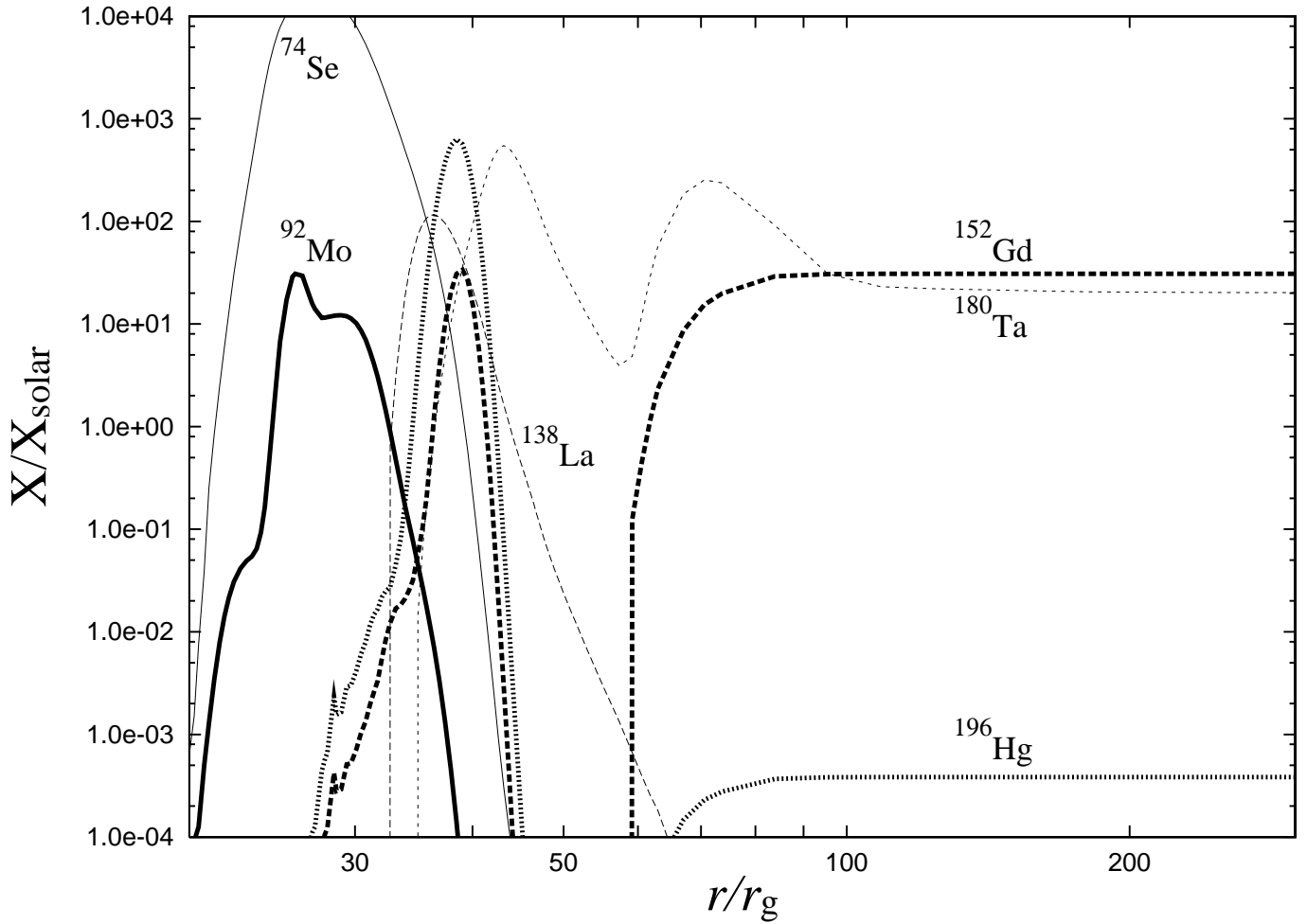


FIG. 2.— The abundance profiles of representative p-nuclei inside a SSAD for M20. The abscissa is the radius of the fallback disk in units of the Schwarzschild radius. The solid, thick-solid, dashed, thick-dashed, dotted, and thick-dotted lines represent ^{74}Se , ^{92}Mo , ^{138}La , ^{152}Gd , ^{180}Ta , and ^{196}Hg , respectively.

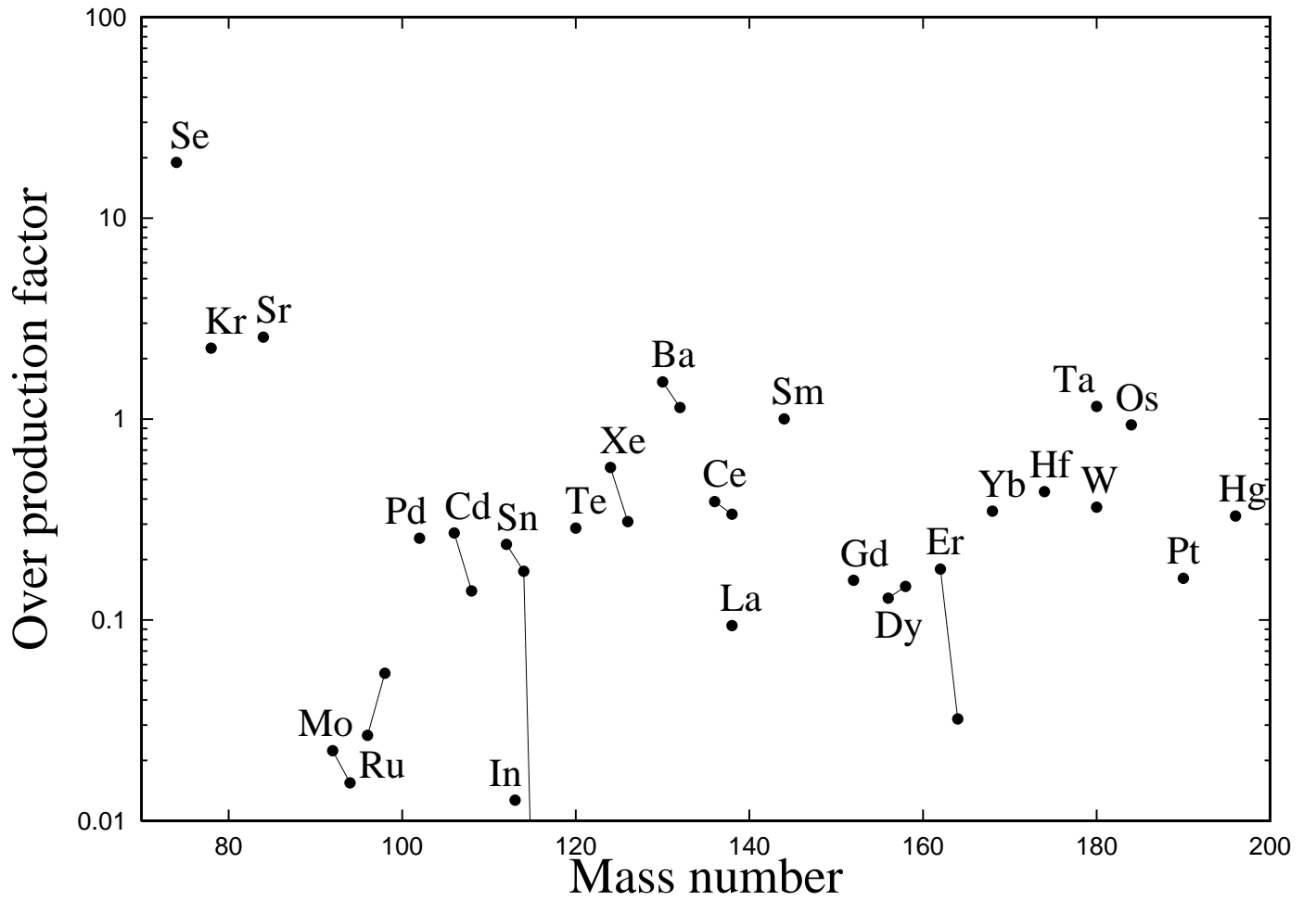


FIG. 3.— OPFs of 35 p-nuclei for M20 with $m = 10^8$. F_0 is equal to 49.64.

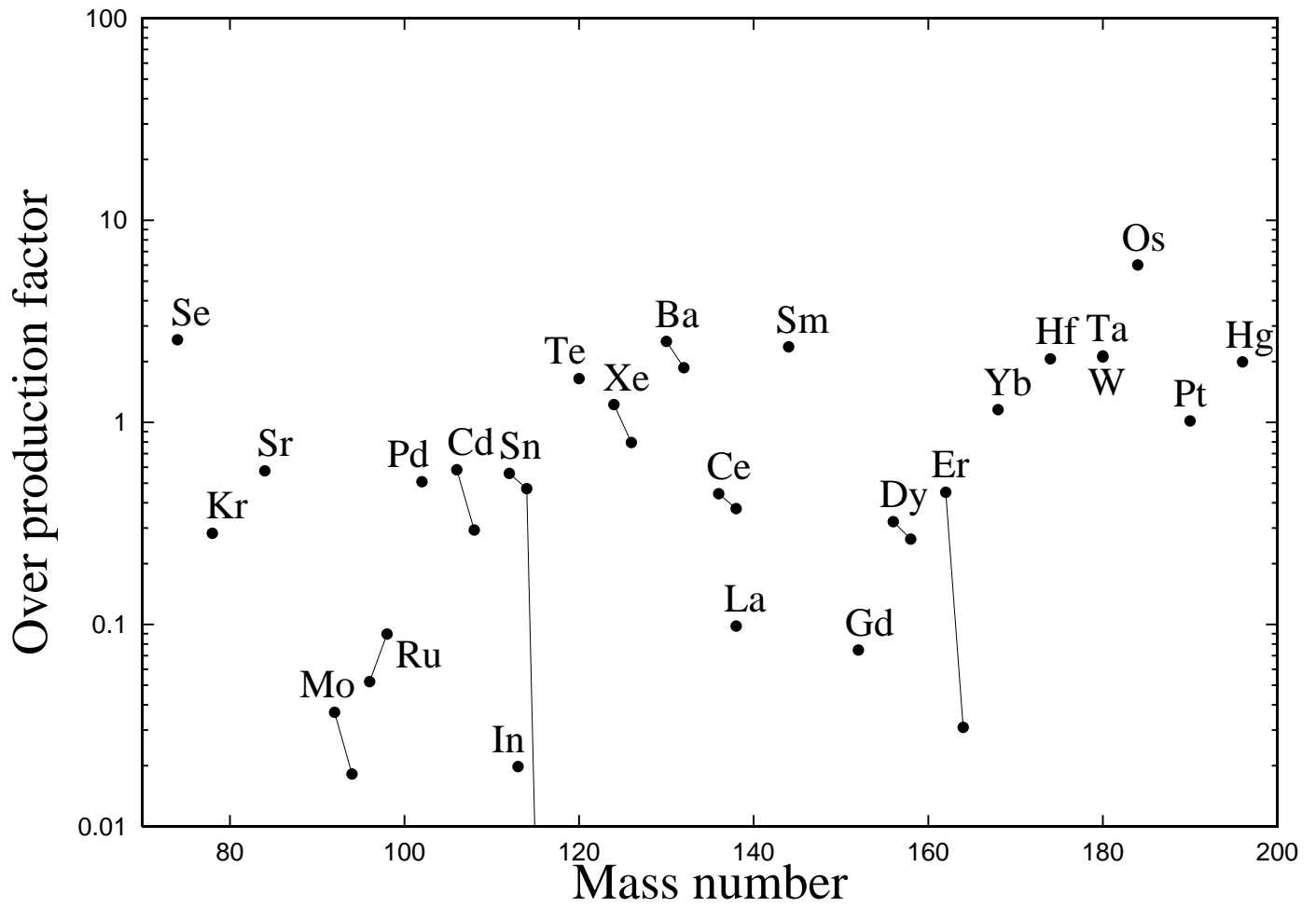


FIG. 4.— Same as figure 3, but for M10. F_0 is equal to 18.51.

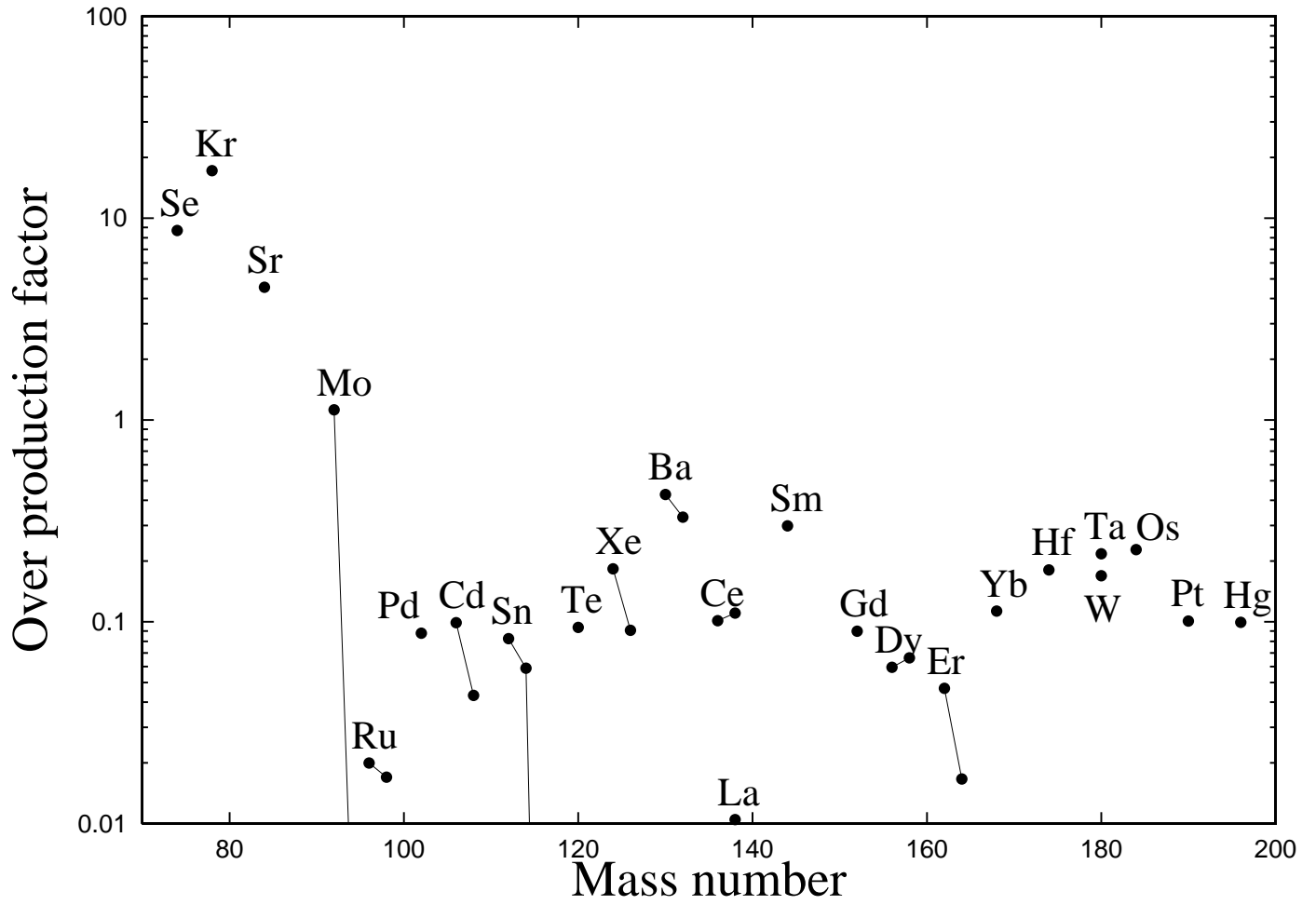


FIG. 5.— Same as figure 3, but for M20P001. F_0 is equal to 157.7.

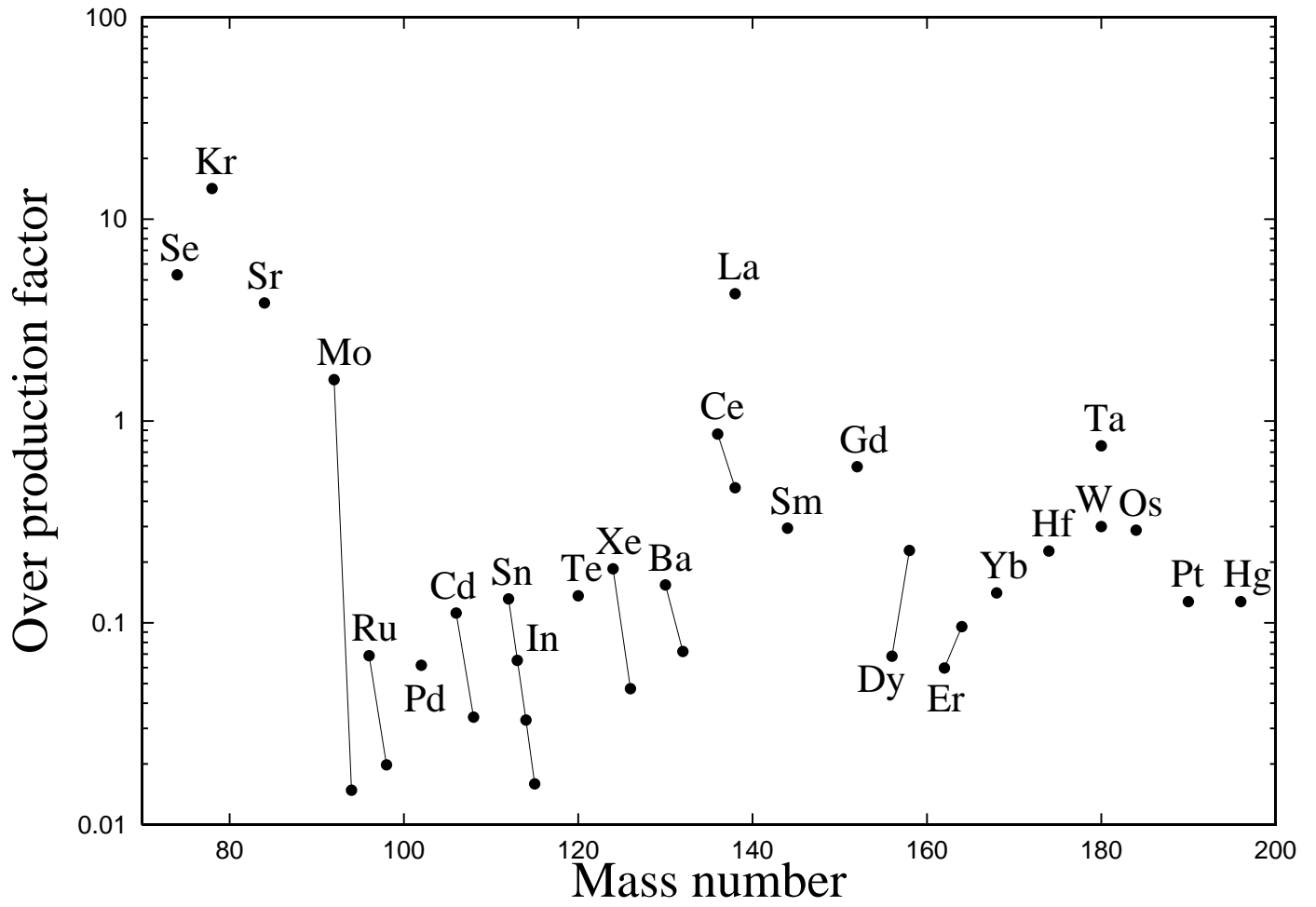


FIG. 6.— OPFs of 35 p-nuclei for M20P01 with $m = 10^6$. F_0 is equal to 41.84

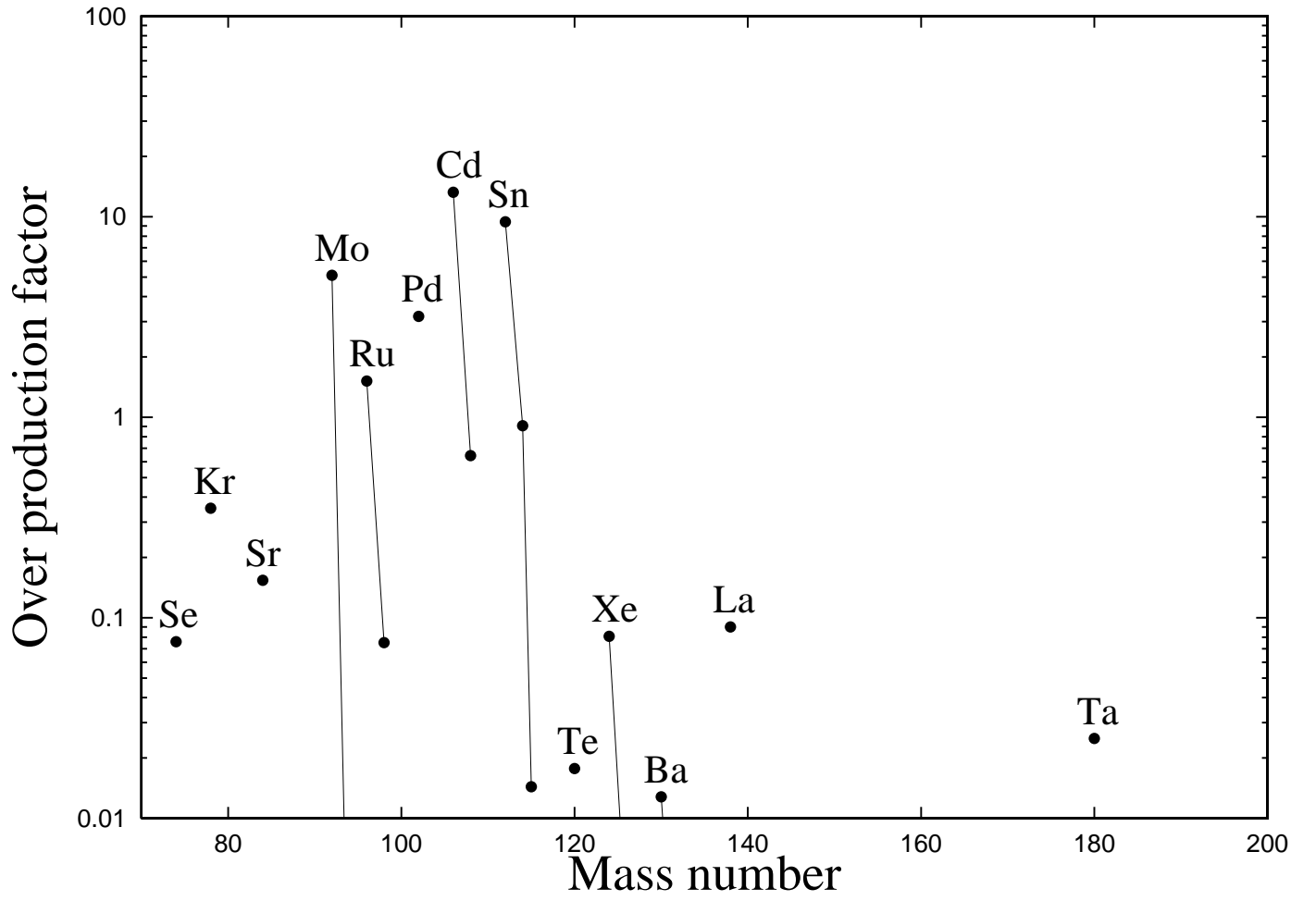


FIG. 7.— Same as figure 6, but for model M20P03. F_0 is equal to 2882